# Simulating Switched Capacitor Circuits With SpectreRF

David Stoops

## I. INTRODUCTION

SWITCHED capacitor circuits have become increasingly popular in recent years. This is due in large part to the availability of the high quality switches provided by CMOS technology. Further, switched capacitor designs have greatly benefited from the substantial developments in the field of digital signal processing. The dependence of filter coefficients on capacitance ratios allows precision on the order of 0.1% in switched capacitor filter implementations. Switched capacitor circuits can also be used to realize circuits such as mixers, voltage controlled oscillators, signal processing circuits, etc.

By their very nature, switched capacitor circuits are time varying. Simulation of such circuits typically requires a transient analysis tool such as HSPICE. In order to obtain a frequency response of a switched capacitor circuit with such a tool, a transient analysis would be required where the time step is determined by the highest frequency and simulation time is determined by the lowest frequency. In addition, some post processing will be required on the output data of the transient analysis to extract gain and phase information. This technique is time consuming and places a high demand on computer resources. If many different frequency response simulations are required to optimize a design such an approach becomes impractical. Mathematical models using tools such as MatLab and MathCad can use z-transform equations to provide transient and frequency responses. However, z-transforms represent an idealized circuit realization that may hide many "real world" limitations of the actual physical implementation of the design such as linearity, clock overlap, dynamic range, etc.

A tool that has been widely used to provide ac analysis of switched capacitor circuits is SwitCap, developed by Columbia University's Department of electrical engineering. Certainly SwitCap has been a useful tool providing quick simulations of switched capacitor circuits in both time and frequency domains. However, in its present form, it is limited to analysis using ideal (linear) elements, and it does not provide noise analysis.

Cadence Design Systems has developed a tool, SpectreRF, a simulator that does time and frequency domain analysis of switched capacitor circuits. Features claimed for the tool include noise analysis, modeling of non-ideal components, distortion analysis, and modeling of periodic time-varying circuits in general, not just switched capacitor circuits.

The purpose of this paper is to provide an introductory tour of SpectreRF while at the same verifying its simulations by comparison with simulations from existing tools. SpectreRF has some striking similarities to SPICE: just as an operating point analysis must be done in SPICE before an ac analysis can be done, SpectreRF requires first computing a periodic operating point using what it calls "Periodic Steady State" analysis (PSS). After the PSS analysis is completed, a "Periodic AC" analysis (PAC) may be run to find the frequency response of the switched capacitor circuit. Noise behavior of the circuit can be simulated with a "Periodic Noise" analysis (Pnoise). This simulation can be used to find the noise referred to the input or to the output of the switched capacitor circuit.

Section II of this paper discusses the circuits used in evaluating SpectreRF. Section III discusses the periodic steady state analysis, and section IV discusses periodic small signal analyses. Section V discusses the simulation of switched capacitor circuits with SpectreRF and compares the results from SpectreRF with Matlab and Switcap.

## II. SWITCHED CAPACITOR LOW PASS FILTERS

The circuits used to demonstrate these analysis tools are shown in Figures 1 and 2. Figure 1 shows the switched capacitor biquad filter used. The transfer function for this circuit is given as

$$H(z) = \frac{0.0108z^2 + 0.0037z + 0.0108}{z^2 - 1.7935z + 0.8203} \tag{1}$$

This circuit has zeros at $z = -0.1694 \pm j0.9855$ and two poles at $z = 0.8968 \pm j0.1272$. It has a DC gain of -0.5dB, 0.5dB ripple in the passband, and a 3dB bandwidth of 1.38MHz when a T=22.2nS (f=45MHz) clock is used. The capacitor

values used are:

$C_1$=170.8fF
$C_2$=0.0fF
$C_3$=13.2fF
$C_4$=180.9fF
$C_5$=180.9fF
$C_6$=219fF
$C_A$=1pF
$C_B$=1pF

A 5th order elliptical filter is also simulated by cascading two biquad filters and a single pole filter. The transfer function that describes this filter is

$$H(z) = \frac{0.0006z^5 - 0.0017z^4 + 0.0011z^3 + 0.0011z^2 - 0.0017z + 0.0006}{z^5 - 4.7345z^4 + 8.9956z^3 - 8.5729z^2 + 4.0975z - 0.7857} \quad (2)$$

The capacitances used for this filter are as follows:

| **Biquad 1** | **Biquad 2** | **Single pole** |
|---|---|---|
| $C_1$=0.1653pF | $C_1$=0.0511pF | $C_1$=-0.0933pF |
| $C_2$=0pF | $C_2$=0pF | $C_2$=0.1866pF |
| $C_3$=0.0969pF | $C_3$=0.0893pF | $C_3$=0.0858pF |
| $C_4$=0.1206pF | $C_4$=0.1525pF | |
| $C_5$=0.1206pF | $C_5$=0.1525pF | |
| $C_6$=0.1274pF | $C_6$=0.0398pF | |

After performing node voltage scaling and capacitance minimization, with a minimum capacitance of 100fF, the capacitances are:

| **Biquad 1** | **Biquad 2** | **Single pole** |
|---|---|---|
| $C_1$=157.1fF | $C_1$=160.8fF | $C_1$=-108.7fF |
| $C_2$=0pF | $C_2$=0pF | $C_2$=217.5fF |
| $C_3$=100.0fF | $C_3$=350.9fF | $C_3$=100.0fF |
| $C_4$=160.1fF | $C_4$=298.4fF | $C_A$=1.166pF |
| $C_5$=249.5fF | $C_5$=383.2fF | |
| $C_6$=211.5fF | $C_6$=100.0fF | |
| $C_A$=1.662pF | $C_A$=1.957pF | |
| $C_B$=1.660pF | $C_B$=2.513pF | |

Transistor models for the TSMC .35μm process are used for the switches. The devices modeled in these examples have a gate width, *W*, of 5*u*m, and a channel length, *L*, of 0.4*u*m. These switches are controlled by a square wave clock that goes from –1.65V to +165V with rise and fall times of 10pS and a period of T=22.2ns.

## III. Periodic Steady State Analysis

A PSS analysis is used to compute the periodic operating point that small signal analyses, such as the periodic AC analysis, will be linearized about. This is the equivalent of computing the DC operating point prior to an AC analysis using SPICE. This analysis must precede any of the other periodic small signal analyses.

The periodic steady state analysis uses a time domain analysis technique called the shooting method. The basis of this technique is that a periodic equation satisfies v(t)=v(t+T), where v(t) is a periodic function, and T is the period. The shooting method finds a set of initial conditions, v(0), that results in steady-state behavior. This is an iterative process that starts with a v(0) and calculates v(T) as well as dv(T)/dv(0), the sensitivity of the final state at time T to the initial state. As shown in [1], the iteration equation formed is

$$v_0^{(r)} = v_0^{(r-1)} - \left[J_\phi(v_0^{(r-1)}) - I\right]^{-1} \cdot \left[\Phi_T(v_0^{(r-1)}, 0) - v_0^{(r-1)}\right] \quad (3)$$

where r is the iteration number, $J_\phi(v_0)$ is the sensitivity, $I$ is the identity matrix, and $\Phi$ is the state transition matrix, with $v(t_1)= \Phi(v(t_0),t_1,t_0)$ and $\Phi_T(v(0),0)= \Phi(v(0),T,t_0)$. This is simply the application of Newton's method to the equation $\Phi_T(v(0),0)=v(0)$.

The function $\Phi_T(v(0),0)$ is the solution to the equation $f(v(t),t)=i(v(t))+dq(v(t))/dt+u(t)=0$ over the interval $t_0$ to $t_0+T$. This equation is typically solved also using the Newton method. This means that the shooting method described, also called the shooting-Newton algorithm, is a multilevel Newton algorithm.

The shooting method has several advantages over other periodic steady state methods, such as harmonic balance. The shooting method is able to handle circuits that are strongly nonlinear. This is because even though the circuit is strongly nonlinear, the function $\Phi_T(v(0),0)$ is usually near linear. This means that the Newton method used to evaluate the periodic operating point will converge in a few iterations. The evaluation of $\Phi_T(v(0),0)$ requires solving the differential equation

$$f(v(t),t) = \frac{dq(v(t))}{dt} + i(v(t)) + u(t) = 0 \tag{4}$$

which may be strongly nonlinear. However, this is done using a transient analysis, which is quite robust. The equation for $f(v(t),t)$ is Kirchov's current law.

The shooting method, since it is based on a transient analysis, is able to handle circuits with inputs that change sharply, such as square waves. During the sharp transition, the transient analysis, used to evaluate $\Phi_T(v(0),0)$, can take smaller time steps to achieve better accuracy. While the circuit is not changing so sharply, the transient analysis is able to take larger time steps, and therefore speed up the simulation.

The disadvantages of the shooting method are that other methods, particularly harmonic balance, are more efficient for smaller, linear circuits. In fact, if a circuit is linear and has sinusoidal currents and voltages, then a harmonic balance analysis is exact, where as the shooting method may not be. However, this is only advantageous for very specific systems. Further, the shooting method has difficulty handling distributed components. With distributed components, the state vector is infinite dimensionally. With a large state vector, the shooting method becomes computationally expensive. Harmonic balance on the other hand, naturally handles such devices. However, in IC analysis, most devices can be represented as lumped devices, and so the shooting method works well.

SpectreRF implements the shooting-Newton algorithm in its periodic steady state analysis. The PSS analysis starts with an initial transient analysis [2]. The transient analysis starts at $t_{start}$ and lasts till $t_{stab}+\max(t_{start},t_{onset})$ where $t_{start}$ is the time at which the transient analysis starts, $t_{onset}$ is the time at which all sources have become periodic, and $t_{stab}$ is additional time that the transient analysis runs. Both $t_{start}$ and $t_{stab}$ are user specified, while $t_{onset}$ is automatically calculated by SpectreRF. After the initial transient analysis, the shooting interval begins. During the shooting interval, SpectreRF implements the shooting-Newton algorithm. The $t_{stab}$ parameter is a user specified parameter that gives Spectre additional time for stabilization. It allows extra time for initial transients to decay or circuit startup. For example, an oscillator requires enough time for the oscillations to grow.

There are other periodic steady state analyses, such as the quasi-periodic steady state analysis and the reader is referred to [1,3] for more information regarding these analyses.

## IV. Periodic Small Signal Analyses

An electrical network can be modeled by Kirchov's current law [1], which is mathematically stated in the equation

$$f(v(t),t) = \frac{dq(v(t))}{dt} + i(v(t)) = e(t) \tag{5}$$

where $v(t)$ are the node voltages, $dq(v(t))/dt$ represents current from charge storing devices, $i(v(t))$ represents currents from conductances, and $e(t)$ represents excitation currents. $f(v(t),t)$ is, in general, a nonlinear, time-varying equation. For periodic circuits, $v(t)$ can be solved with methods such as the shooting method, which was discussed in section III. If the solution to $f(v(t),t)$ for a specific, periodic input, $e_o(t)$, and a specific circuit that is periodic with a commensurate period to $e_o(t)$, is denoted $v_o(t)$, then $f(v(t),t)$ can be expanded into a series about the solution $v_o(t)$. This is written as

$$f\left(v(t),t\right)=f\left(v_0(t),t\right)+\sum_{n=1}^{\infty}\frac{1}{n!}\left.\frac{\partial^n f\left(v(t),t\right)}{\partial v(t)^n}\right|_{v(t)=v_o(t)}\left(v(t)-v_o(t)\right)^n \tag{6}$$

Noting that $f(v_o(t),t)=e_o(t)$, equation (6) can be rewritten as

$$\Delta e(t)=e(t)-e_o(t)=\sum_{n=1}^{\infty}\frac{1}{n!}\left.\frac{\partial^n f\left(v(t),t\right)}{\partial v(t)^n}\right|_{v(t)=v_o(t)}\left(v(t)-v_o(t)\right)^n \tag{7}$$

Under small signal conditions, $v(t)-v_o(t)$ is a small quantity, and $(v(t)-v_o(t))^n$ is negligible for $n>1$. This leads to the small signal approximation, specifically

$$\Delta e(t)=\left.\frac{\partial f\left(v(t),t\right)}{\partial v(t)}\right|_{v(t)=v_o(t)}\Delta v(t) \tag{8}$$

where $\Delta v(t)=v(t)-v_o(t)$. Clearly equation (8) is a linear equation of $\Delta v(t)$. In deriving equation (8), the assumption was made that $(v(t)-v_o(t))$ is a small quantity. This is true if $v_o(t)$ is a large signal, and $v(t)\sim v_o(t)$, in other words, $v(t)$ is a perturbation of $v_o(t)$. Equation (8) can be rewritten as

$$\Delta e(t)=\frac{d}{dt}\left(\left.\frac{dq(v(t))}{dv(t)}\right|_{v(t)=v_o(t)}\right)\Delta v(t)+\left.\frac{di(v(t))}{dv}\right|_{v(t)=v_o(t)}\Delta v(t)=\frac{dC_o(t)}{dt}\Delta v(t)+G_o(t)\Delta v(t) \tag{9}$$

Since the large signal excitation, $e_o(t)$ is periodic and the system responds in a periodic manner, with a period that is commensurate with $e_o(t)$, $v_o(t)$ is periodic as well. If the period of $v_o(t)$ it $T_o$, then $dC_o(t)/dt$ and $G_o(t)$ are periodic with period $T_o$. This is shown as

$$C_o(t+T_o)=\left.\frac{dq(v(t))}{dv(t)}\right|_{v(t)=v_o(t+T_o)}=\left.\frac{dq(v(t))}{dv(t)}\right|_{v(t)=v_o(t)}=C_o(t) \tag{10}$$

If $C_o(t)$ is periodic with period $T_o$, then so is it's time derivative. A similar proof can show that $G_o(t)$ is periodic with period $T_o$.

Equation (9) is a periodically time-varying, linear system in $\Delta v(t)$. Since the system is linear and periodic, $\Delta v(t)$ is, when excited by the complex exponential $U_s e^{j\omega_s t}$, a sum of complex exponentials given by [1,4,5]

$$\Delta v(t)=\sum_{n=-\infty}^{\infty}V_n e^{j(\omega_s-n\omega_o)t} \tag{11}$$

where $\omega_o=2\pi/T_o$ is the fundamental frequency of the periodic steady state, $v_o(t)$. This result is proved in appendix A. As (11) shows, there are output tones at $\omega_s-n\omega_o$. These are sidebands produced by the time-varying nature of the system.

Taking equation (11) and evaluating at $t=t+T_o$

$$\Delta v(t+T_o)=\sum_{n=-\infty}^{\infty}V_n e^{j(\omega_s-n\omega_L)(t+T_o)}=e^{j\omega_s T_o}\sum_{n=-\infty}^{\infty}V_n e^{j(\omega_s-n\omega_o)t}=\Delta v(t)e^{j\omega_s T_o} \tag{12}$$

Equation (12) shows that a complete solution for $\Delta v(t)$ over all time can be derived from the solution of $\Delta v(t)$ over any time interval of $T_o$. Furthermore, equation (12) can be rewritten as

$$\Delta v(t+T_o)-\Delta v(t)e^{j\omega_s T_L}=0 \tag{13}$$

Equation (13) can be solved using the shooting method described in section III [1]. There are other methods, such as harmonic balance that can solve equation (13) as well.

Once $\Delta v(t)$ is solved for over an interval $T_o$, the Fourier coefficients, $V_n$, in equation (11) can be solved for using methods such as the discrete Fourier transform or the Fourier integral. The transfer function from the input to the output at sideband n is then given as

$$H_n(j\omega_s) = \frac{V_n}{U_s} \tag{14}$$

The small signal frequency can be swept, and the $H_n(j\omega_s)$ can be calculated at the frequency points of interest. In this manner the frequency response can be calculated for the system. This analysis computes the response from a source to every node in the system, and is called a periodic AC analysis.

An extension of the periodic AC analysis is the periodic transfer function analysis. This analysis computes the transfer function from every source in the circuit at the sidebands of interest to the output at the baseband frequency. This analysis is a periodic AC analysis computed on the adjoint network [3,6,7].

The periodic noise analysis is another small signal analysis that computes the noise power from the components in a circuit to the output. The periodic noise analysis uses an adjoint network to compute the transfer function from all noise sources at all sidebands to the output at the baseband. The output noise can then be calculated as

$$S_{out}(\omega) = \sum_{i=1}^{N} |H_i(j\omega)|^2 S_i(\omega) \tag{15}$$

where $S_i(\omega)$ is the power spectral density of noise source i, and $H_i(j\omega)$ is the transfer function from noise source i to the output. The noise produced from a time-varying system is typically cyclostationary in nature.

The key assumption made in deriving the results in this section is that the system can be approximated by the first order term in the power series. This assumption implies that the output is a near linear relationship to the input. Another assumption made in these derivations is that the system responds periodically to a large signal periodic input.

There are other small signal analyses as well, such as the periodic s parameter analysis. The reader is referred to [2,3,8] for more information on other small signal analyses.

## V. Simulation of Switched Capacitor Circuits

As mentioned in the introduction, switched capacitor circuits are difficult to simulate due to their time varying nature. During one clock phase, the capacitors are switched to a charging position, and during another clock phase, they are switched to a discharging position. SpectreRF is able to simulate these circuits with its periodic steady state analysis and periodic small signal analyses.

The switched capacitor circuit is driven by a large signal, the clock. The clock is used to turn on and off switches, which are typically MOSFETs. The circuit responds in a strongly nonlinear manner to the clock. The switched capacitor circuit is also driven by an input signal. The circuit is designed to respond in a linear fashion to the input signal. This situation represents a periodically varying system that SpectreRF can simulate.

In order to simulate this circuit, the input signal should be set to zero, and the a periodic steady state analysis should be run with the clock alone driving the circuit. After the periodic steady state solution has been calculated, the input signal should be applied, and a periodic AC analysis can be run. This will give the frequency response of the switched capacitor circuit. In doing this analysis, several assumptions have been made. The first assumption is that the switched capacitor circuit responds in a periodic manner to the clock. This assumption is obviously true. The effect of the clock on the switched capacitor circuit is to change the conductances of the switches, either turn on the transistors, or turn them off. The signal path is defined by the transistors that turn on. Since the clock is periodic, the signal path in the circuit will be periodic. This means that the circuit will respond in a periodic manner with the same period as the clock. Another assumption made concerning the periodic steady state analysis is that the periodic response is a near linear function. This assumption is also true. With no input applied, there is no source to charge the capacitors. Since no capacitors are charging, the state of the circuit will be the same at the beginning and end of the period. These are the only assumptions made concerning the periodic steady state analysis. The small signal analyses makes another assumptions about the circuit. The assumption is that the circuit responds linearly to the input. Switched capacitor circuits are typically designed to do this. Thus this assumption is true by design.

The circuits presented in section II were simulated in SpectreRF and Switcap. The circuit transfer functions were used in Matlab to computer the ideal frequency response. Figures 3-4 show the SpectreRF results of the biquad filter and the 5$^{th}$ order elliptical

filter respectively. These graphs were imported into Matlab, and compared against the results from Switcap and Matlab. These comparisons are shown in Figures 5-8 respectively. As the graphs show, there is good agreement between Switcap, Matlab, and SpectreRF.

Figures 9 and 10 show the results of a periodic noise analysis for the biquad filter and the $5^{th}$ order elliptical filter. As the graph shows, the noise in the circuit consists of white noise that has been shaped by the filter. It is obvious from the graph that flicker noise has not been incorporated into the transistor model. There is also some peaking around the cutoff frequency. The graphs also show the effect of the number of sidebands used in the noise calculations. The periodic noise analysis takes into account the noise folding due to the time-varying nature of the circuit. Therefore, the more sidebands used in the calculation, the more accurate the answer will be. However, the accuracy increases little after so many sidebands are taken into account.

Another capability of SpectreRF is its ability to calculate distortion. The method used to calculate distortion is to run a quasiperiodic steady state analysis. In the quasiperiodic steady state analysis, one large signal is applied and multiple moderate tones are applied to the circuit. The steady state is then calculated, and the output tones can be displayed. Figure 11 shows the results of such an analysis when a 1V sinusoid with a frequency of 100KHz is applied to the input. As can be seen, there are tones at multiples of the fundamental.

## VI. Conclusion

This paper has compared several methods to simulate switched capacitor circuits, including a new tool, SpectreRF, aimed specifically at RF and switched capacitor circuit simulations. It has also described some of the theory behind the SpectreRF simulator. Two switched capacitor filters have been simulated in order to demonstrate the SpectreRF analyses. The paper also verified that the switched capacitor filters simulated did not violate the assumptions made in the derivation of the simulation algorithms. The results were presented, and the transfer functions obtained by SpectreRF were compared to those obtained from Switcap and Matlab. The results were in close agreement showing that SpectreRF provides valid simulation results for AC analysis. This paper has validated some of the theory and math behind SpectreRF, but has not verified these results with physical circuits. SpectreRF's simulations would have to be verified by comparison with actual circuit results, which is beyond the scope of this paper.

**References**


[1] K. Kundert. Simulation Methods for RF Integrated Circuits. *Proceedings of ICCAD*. November 1997.

[2] Affirma RF Simulator (SpectreRF) Theory. Cadence Design Systems.

[3] K. Kundert. Introduction to RF Simulation and Its Application. *IEEE J Solid-State Circuits*. vol. 34, pp. 1298-1319, September 1999.

[4] M. Okumara, T. Sugawara, H. Tanimoto. An Efficient Small Signal Frequency Analysis Method of Nonlinear Circuits with Two Frequency Excitations. *IEEE Trans. On Computer-Aided Design*. vol. 9, pp. 225-235, March 1990

[5] L. Zadeh. Frequency Analysis of Variable Networks. *Proc. IRE*. vol 32, pp. 291-299, 1950.

[6] F. Yuan, A. Opal. Adjoint Network of Periodically Switched Linear Circuits with Applications to Noise Analysis. *IEEE. Trans. on Circuits and Systems-I: Fundamental Theory and Applications.* vol 48, pp. 139-151, February 2001.

[7] A. Opal, J. Vlach. Adjoint Network of Periodically Switched Linear Circuits. *IEEE.* VI-298 - VI-301, 1998.

[8] Affirma RF Simulator (SpectreRF) User Guide. Cadence Design Systems.

[9] SwitCap, www.cisl.columbia.edu/projects/switcap.

[10] Matlab, www.mathworks.com.

[11] J. Phillips, K. Kundert. Noise in mixers, oscillators, samplers, and logic: an introduction to cyclostationary noise. www.designers-guide.com/Theory

[12] K. Kundert. Simulating Switched-Capacitor Filters with SpectreRF. www.designers-guide.com/Analysis.

[13] A. Opal, J. Vlach, Analysis and Sensitivity of Periodically Switched Linear Networks. *IEEE Trans. On Circuits and Systems*. vol. 36, pp. 522-532, April 1989.

[14] M. Gourary, S. Rusakov, S. Ulyanov, M. Zharov. A New Simulation Technique for Periodic Small-Signal Analysis. *IEEE*. 2003

[15] R. Telichevesky, K. Kundert, I. Elfadel, J. White. Fast Simulation Algorithms for RF Circuits. *IEEE Custom Integrated Circuits Conference.* Pp. 21.1.1-21.1.8, 1996.

[16] R. Telichevesky, K. Kundert. Efficient AC and Noise Analysis of Two-Tone RF Circuits. *33rd Design Automation Conference*. 1996.

[17] R. Telichevesky, K. Kundert. Receiver Characterization using Periodic Small-Signal Analysis. *IEEE Custom Integrated Circuit Conference*. 1996.

[18] K. Kundert, A. Sangiovanni-Vincentelli. Finding the Steady-State Response of Analog and Microwave Circuits. *IEEE*

*Custom Integrated Circuit Conference*. 1988.
[19] K. Kundert, I. Clifford. Achieving Accurate Results with a Circuit Simulator. *Cadence Design Systems.*

[20] H. D'Angelo. *Linear Time-Varying Systems: Analysis and Synthesis*. Allyn and Bacon Series in Electrical Engineering. 1970.
[21] K. Martin, D. Johns. *Analog Integrated Circuit Design*. John Wiley & Sons. 1997
[22] K. Kundert. Accurate Fourier Analysis for Circuit Simulators, *IEEE Custom Integrated Circuit Conference*. 1994.
[23] K. Mayaram, D. Lee, S. Moinian, D. Rich, J. Roychowdhury. Computer-Aided Circuit Analysis Tools for RFIC Simulation: Algorithms, Features, and Limitations. *IEEE Trans. On Circuits and Systems II: Analog and Digital Signal Processing*. vol 47, pp. 274-286, April 2000.

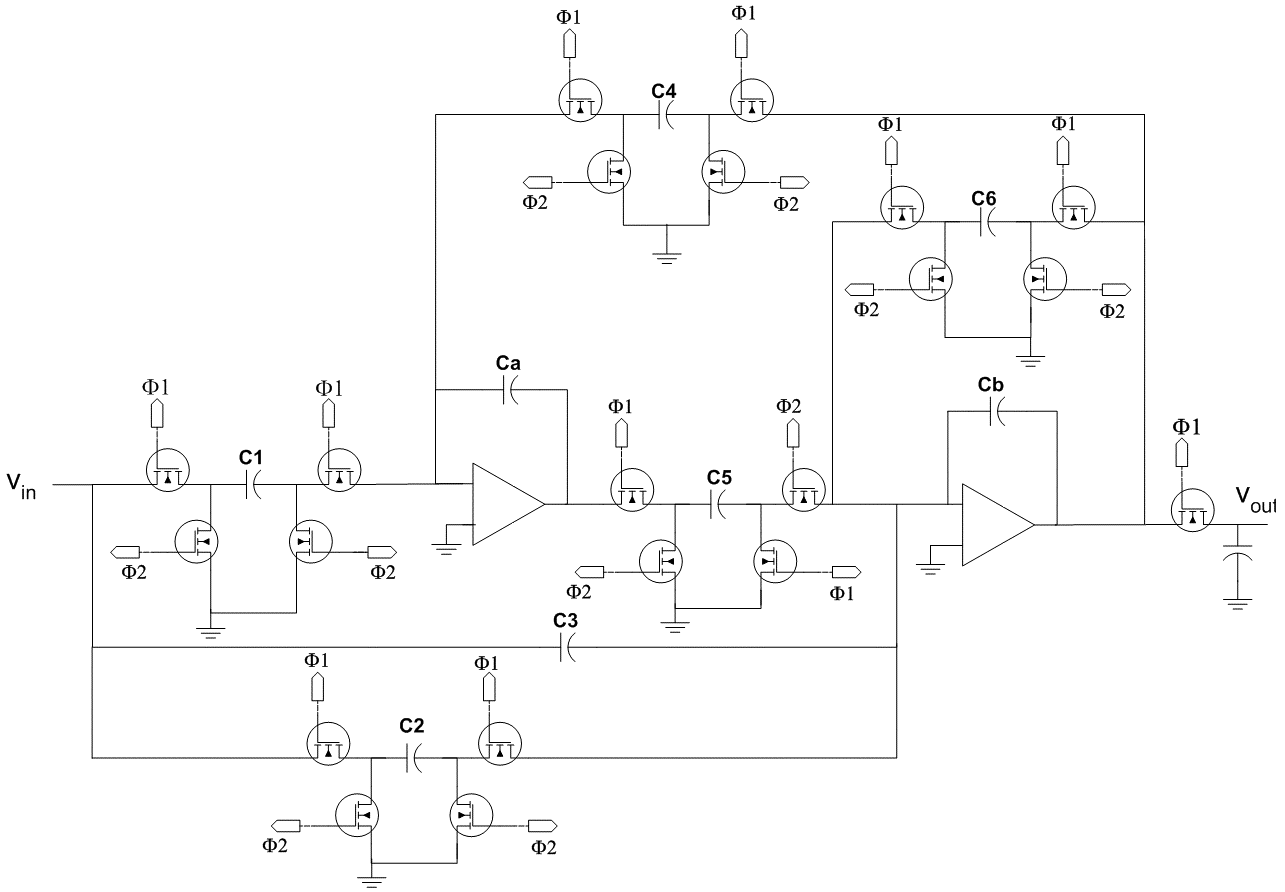


**Figure 1. Low pass switched capacitor biquad filter**

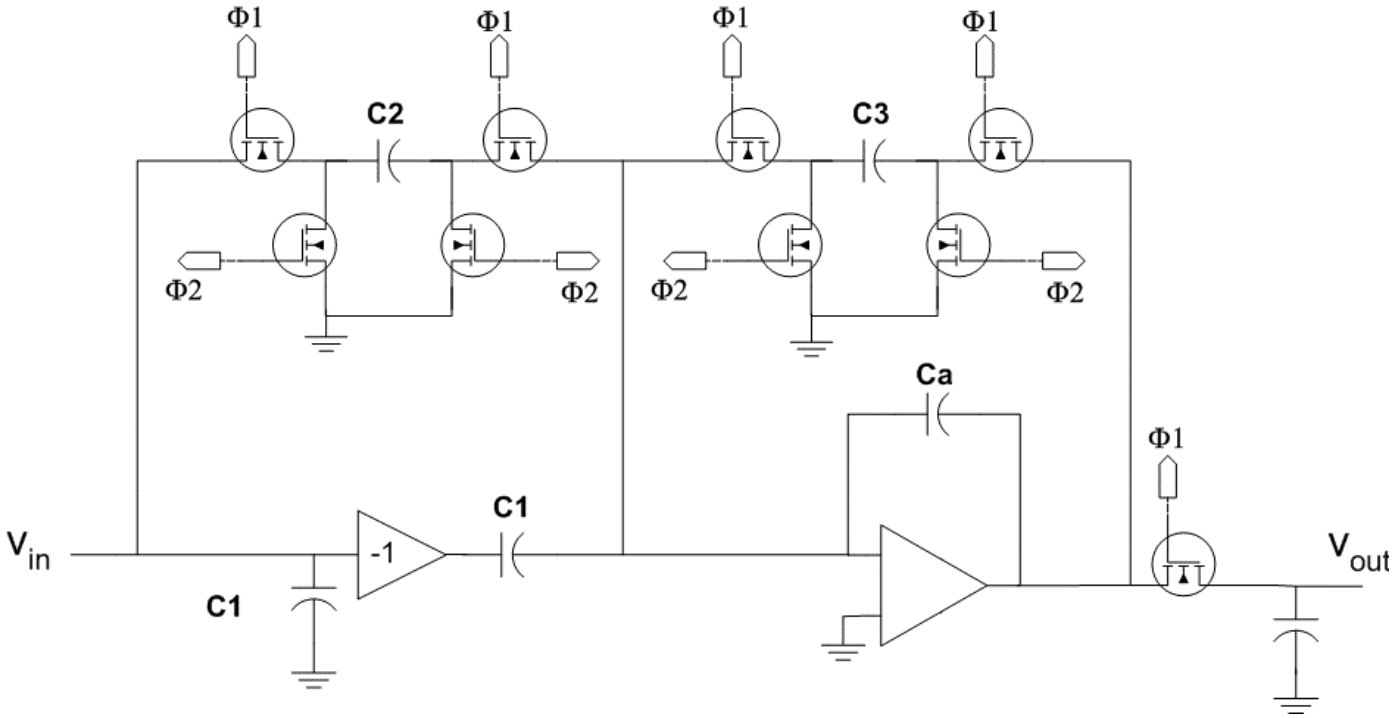


**Figure 2. Low pass single pole switched capacitor filter**

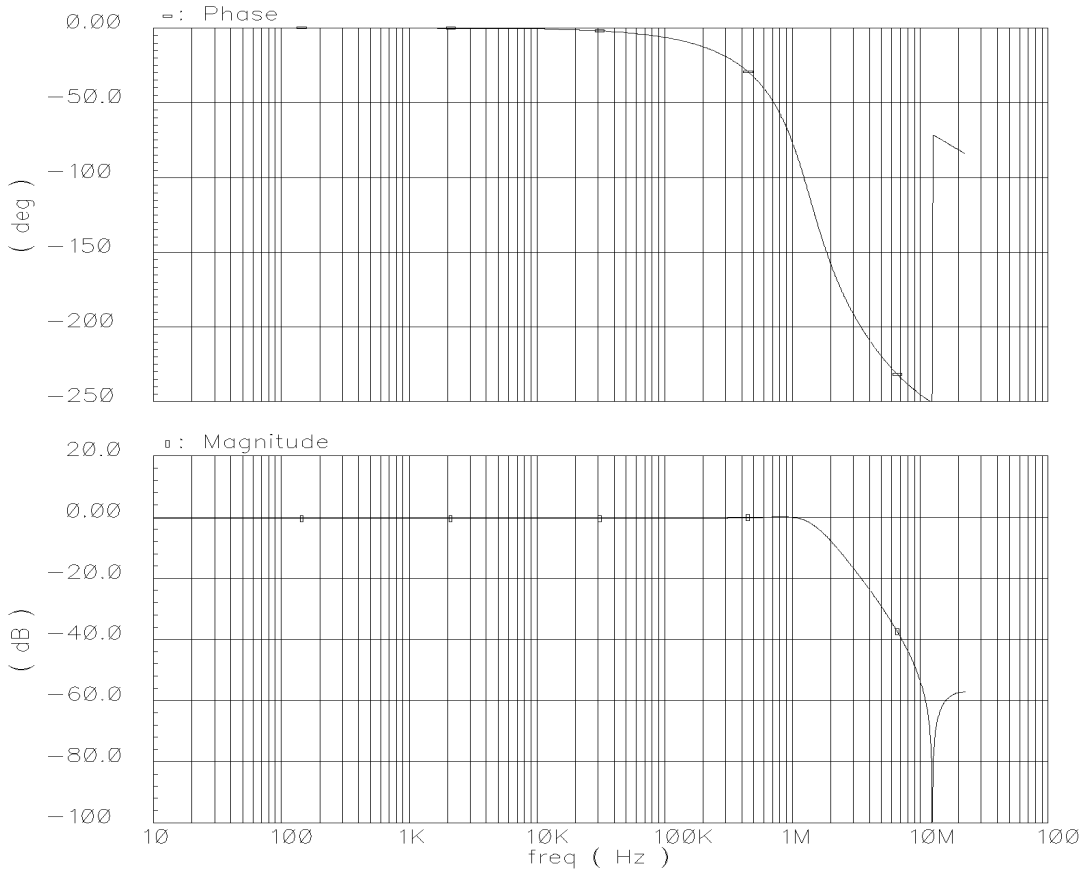


**Figure 3. SpectreRF simulation results for a biquad switched capacitor filter.**

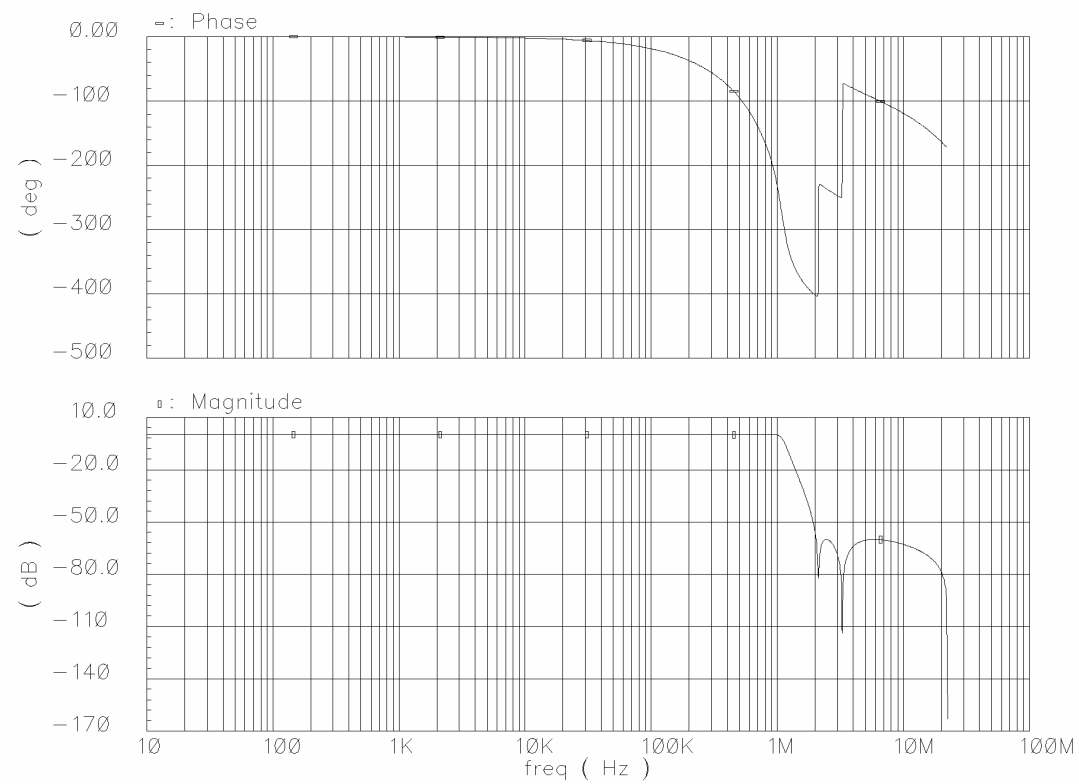


**Figure 4. SpectreRF simulation results for a 5th order elliptical switched capacitor filter.**

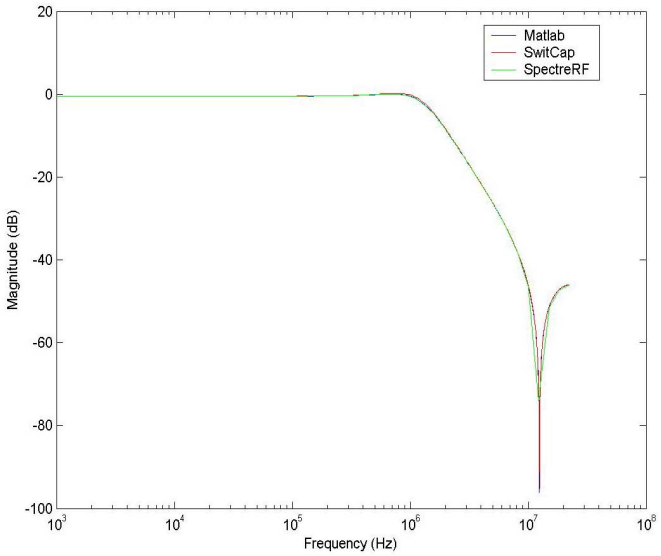


**Figure 5. Comparison of biquad magnitude transfer function of SpectreRF, Switcap, and Matlab.**

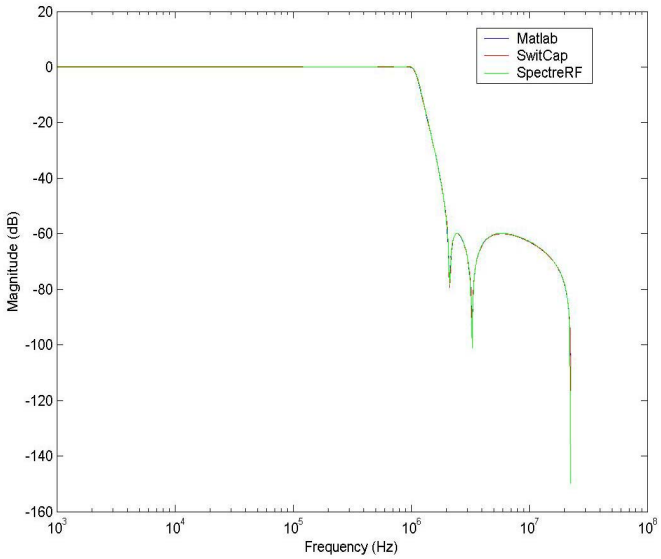


**Figure 7. Comparison of 5th order elliptical filter magnitude transfer function of SpectreRF, Switcap, and Matlab.**

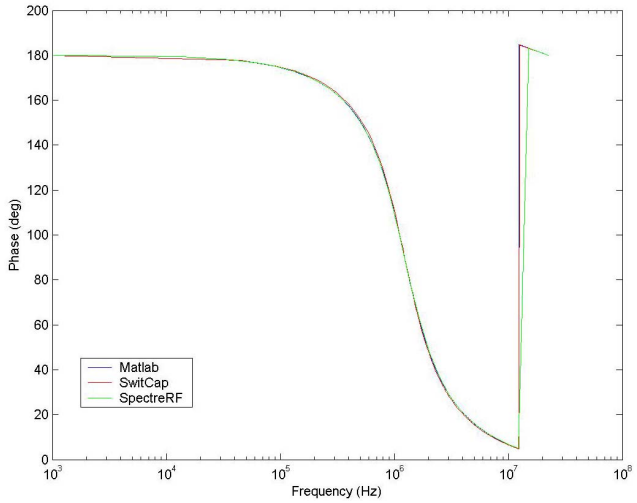


**Figure 6. Comparison of biquad phase transfer function of SpectreRF, Switcap, and Matlab.**

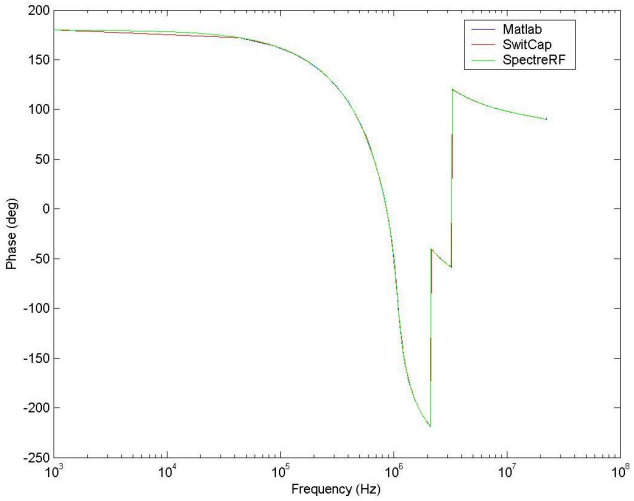


**Figure 8. Comparison of 5th order elliptical filter phase transfer function of SpectreRF, Switcap, and Matlab**

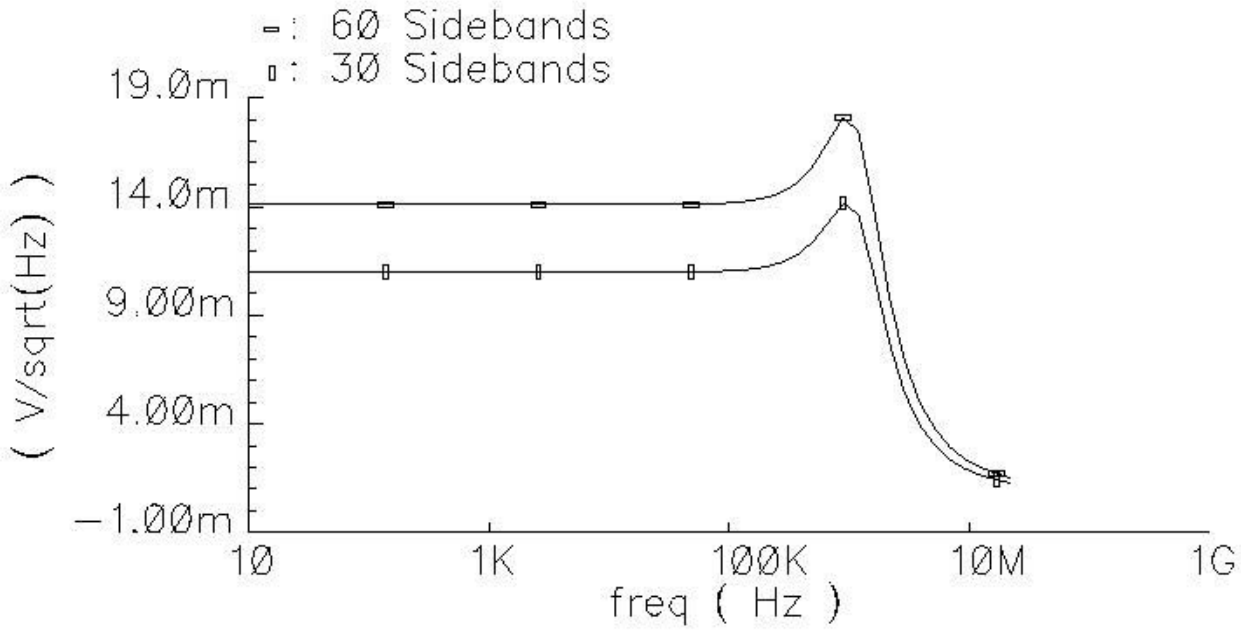


**Figure 9. Output noise of the biquad filter.**

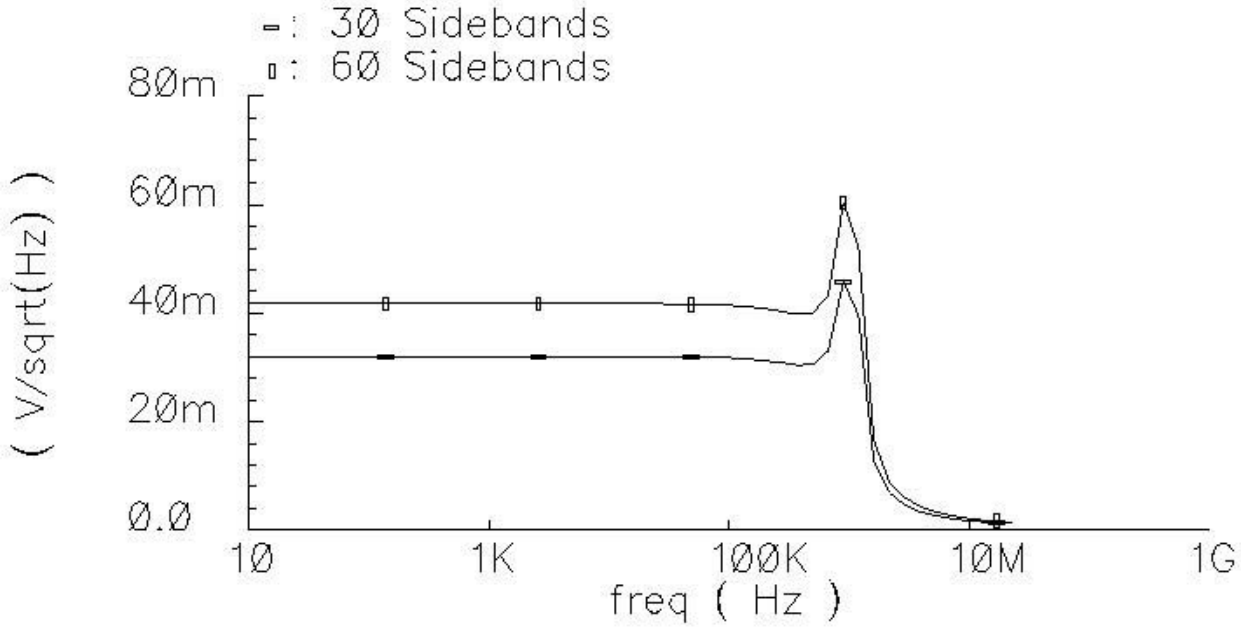


**Figure 10. Output noise of a 5th order elliptical filter.**

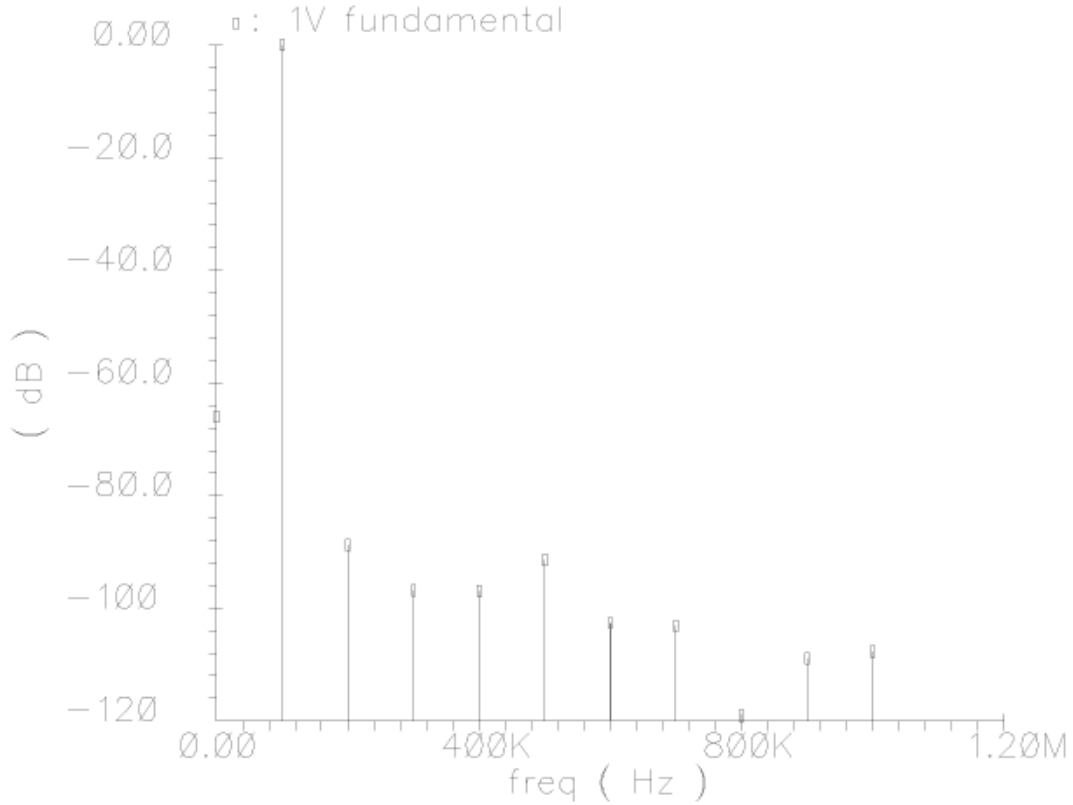


**Figure 11. Results of the quasi-periodic steady state analysis. The distortion components are shown at multiples of the 100KHz fundamental.**

**Appendix A**

The goal of this appendix is to show that a periodically varying linear system responds to a complex exponential input with a series of complex exponential outputs. The proof starts by showing that convolution with the impulse response in the time domain translates to multiplication with the system function in a transformed domain. The proof then uses the Fourier transform kernel to analyze an arbitrary periodically varying system. The proof shows that a periodically varying impulse response will result in a periodically varying system function in the Fourier domain. The system function is then turned into a Fourier series. It is then shown that the system, when excited by a complex exponential, will result in a series of complex exponentials at the output.

The integral transform is defined as

$$F(\lambda)=\int_{a}^{b} f(t)K(t,\lambda)dt \tag{1}$$

where K(t,λ) is the kernel of the transformation and λ is the variable of the transformed domain. The inverse integral transform is given as

$$f(t)=\frac{1}{j2\pi}\int_{C} F(\lambda)k(t,\lambda)d\lambda \tag{2}$$

where k(t,λ) is the inverse transform kernel and C is an appropriately chosen contour in the λ-domain.

A linear system's output is related to its input through the convolution integral. This is shown as

$$y(t)=\int_{-\infty}^{\infty} h(t,\tau)x(\tau)d\tau \tag{3}$$

Using equation (2) to replace x(τ) in equation (3), y(t) can be written as:

$$y(t)=\int_{-\infty}^{\infty} h(t,\tau)\left[\frac{1}{j2\pi}\int_{C} F(\lambda)k(\tau,\lambda)d\lambda\right]d\tau \tag{4}$$

If the order of integration is changed, then y(t) is

$$y(t)=\frac{1}{j2\pi}\int_{C} F(\lambda)\left[\int_{-\infty}^{\infty} h(t,\tau)k(\tau,\lambda)d\tau\right]d\lambda \tag{5}$$

But the inner integral in (5) can be rewritten as follows

$$y(t)=\frac{1}{j2\pi}\int_{C} F(\lambda)\left[\frac{k(t,\lambda)}{k(t,\lambda)}\int_{-\infty}^{\infty} h(t,\tau)k(\tau,\lambda)d\tau\right]d\lambda=\frac{1}{j2\pi}\int_{C} F(\lambda)k(t,\lambda)G(\lambda,t)d\lambda \tag{6}$$

where G(λ,t) is defined as

$$\left[\frac{1}{k(t,\lambda)}\int_{-\infty}^{\infty} h(t,\tau)k(\tau,\lambda)d\tau\right] \tag{7}$$

It can be easily seen that if the system is stimulated by an input signal equal to the inverse kernal, k(t,λ), then G(t,λ) is the output response of the system divided by the inverse kernal; that is,

$$G(\lambda,t)=\left.\frac{y(t)}{x(t)}\right|_{x(t)=k(t,\lambda)} \tag{8}$$

In this definition, λ is treated as an input parameter.

Equation (6) shows that the output is equal to inverse transform of the system function multiplied by the transformed input. This means that the input/output relationship of convolution in the time domain turns into multiplication in the transformed domain.

An interesting point to be noted in the derivation of equation (6) is that no restriction has been placed on the system other than it has to be linear.

If the inverse transform kernel is chosen to be $e^{j\omega t}$, then $\lambda=j\omega$ and the inverse transform is the inverse Fourier transform. With that particular inverse transform kernel, the transform kernel is $e^{-j\omega t}$. With this transform, the system function in equation (7) becomes:

$$G(j\omega,t)=\int_{-\infty}^{\infty}h(t,\tau)e^{-j\omega(t-\tau)}d\tau \tag{9}$$

If $h(t,\tau)$ is periodic, then it remains unchanged by a shift of a period. This means that

$$h(t+nT,\tau+nT)=h(t,\tau) \tag{10}$$

If $h(t,\tau)$ is periodic, then under the Fourier transform, $G(j\omega,t)$ is periodic with respect to t. This is shown as

$$G(j\omega,t+nT)=\int_{-\infty}^{\infty}h(t+nT,\tau)e^{-j\omega(t+nT-\tau)}d\tau \tag{11}$$

Choose $\tau=u+nT$ and $d\tau=du$, then equation (11) becomes

$$G(j\omega,t+nT)=\int_{-\infty}^{\infty}h(t+nT,u+nT)e^{-j\omega(t+nT-u-nT)}du \tag{12}$$

Using equation (10), equation (12) can be rewritten as

$$G(j\omega,t+nT)=\int_{-\infty}^{\infty}h(t,u)e^{-j\omega(t-u)}du=G(j\omega,t) \tag{13}$$

Equation (13) shows that a periodic impulse response produces a periodic system function when the Fourier transform kernel is used. Since $G(j\omega,t)$ is periodic with respect to t, it can be expanded into a Fourier series. Therefore, a periodic system function can be written as

$$G(j\omega,t)=\sum_{n=-\infty}^{\infty}g_n(\omega)e^{-j\frac{2\pi}{T_L}nt} \tag{14}$$

If an input of $e^{j\omega_s t}$ is applied to a linear system, then, using the relationship from equation (6) the output can be written as

$$y(t)=\frac{1}{2\pi}\int_{-\infty}^{\infty}G(j\omega,t)\delta(\omega-\omega_s)e^{j\omega t}d\omega \tag{15}$$

where $\delta(\omega-\omega_s)$ is the Fourier transform of the complex exponential. The integral of equation (15) can be evaluated and y(t) becomes

$$y(t)=\frac{1}{2\pi}G(j\omega_s,t)e^{j\omega_s t} \tag{16}$$

If $G(j\omega,t)$ describes a periodic system, then equation (14) can be substituted in equation (16) and the output can be shown to be

$$y(t)=\frac{1}{2\pi}\sum_{n=-\infty}^{\infty}g_n(\omega_s)e^{-j\frac{2\pi}{T_L}nt}e^{j\omega_s t} \tag{17}$$

Since $g_n(\omega_s)$ is a constant, and $2\pi/T_L$ can be written as $\omega_L$, equation (17) can be rewritten as

$$y(t) = \sum_{n=-\infty}^{\infty} a_n e^{j(\omega_s - n\omega_L)t} \tag{18}$$

Equation (18) shows that a periodically time-varying system with a complex exponential input at frequency $\omega_s$ will produce outputs at tones $\omega_s, \omega_s \pm \omega_L, \omega_s \pm 2\omega_L, \ldots$

Equation (18) shows that a periodically varying system with a complex exponential input produces a series of complex exponentials at the output.